



## One pot spontaneous green synthesis of gold nanoparticles using *Cocos nucifera* (coconut palm) coir extract

Harshala Parab\*, Niyoti Shenoy, Sanjukta A. Kumar,  
Sangita D. Kumar and A.V.R. Reddy

Analytical Chemistry Division, Bhabha Atomic Research Centre, Trombay, Mumbai- 400085.

Received 09 Aug 2015, Revised 06 Nov 2015, Accepted 24 Nov 2015

\*Corresponding Author. E-mail: [harshprb@gmail.com](mailto:harshprb@gmail.com), [harshala@barc.gov.in](mailto:harshala@barc.gov.in); Tel: (+91-2225592238)

### Abstract

A spontaneous, one-pot strategy for the room temperature synthesis of gold nanoparticles (AuNPs) using *Cocos Nucifera* Linn (coconut palm) coir extract is described. The formation of AuNPs was observed within 30s of reaction time between the metal precursor and coir extract. The bioextract acted as both reducing agent and a stabilizer. The influence of various experimental parameters such as % volume fraction of coir extract, concentration of metal precursor, contact time and solution pH on the formation of AuNPs was evaluated to determine the optimum conditions for synthesis. As synthesized AuNPs were characterized by UV-Vis spectroscopy, X-ray diffraction (XRD), transmission electron microscopy (TEM), energy dispersive X-ray analysis (EDAX), Fourier transform infra red spectroscopy (FTIR) and electrophoretic mobility measurements. The analyses indicated the formation of spherical, crystalline, nanometer-sized particles carrying negative surface charge due to the presence of various functional groups from coir extract. The possible mechanism of the formation and stabilization of AuNPs is discussed. The catalytic activity of AuNPs for the reduction of 4-nitrophenol (4-NP) to 4-aminophenol (4-AP) in the presence of sodium borohydride was investigated. Moreover, the present synthetic strategy can be extended to prepare the nanoparticles of other metal ions such as silver and platinum.

**Keywords:** one-pot strategy; synthesis; gold nanoparticles (AuNPs); coir extract; catalytic activity

### 1. Introduction

Metal nanoparticles (MNPs) especially gold have attracted considerable attention as compared to their bulk counterparts due to their wide potential applications in catalysis, biosensing, biomedicines, micro-electronics etc. [1-3]. A large number of methods for the preparation of gold nanoparticles (AuNPs) have been reported in the literature. The most common methods involve reduction of gold precursor in liquid phase using reducing agents such as sodium citrate, sodium borohydride, and hydrogen [4-7]. However colloidal particles with small size possess the tendency to aggregate in liquid phase. To circumvent this aggregation, capping agents such as surfactants or polymers are used to obtain a stable dispersion of nanoparticles (NPs) in liquid phase. Considering the toxicity of different reagents used in the synthesis, there is a growing need for the development of simple, non-toxic and environmentally benign synthetic protocols. Over the past two decades, many attempts have been made for the green synthesis of nanoparticles. Bio-based synthetic strategies are attractive in this

view, since they meet most of the requirements mentioned above. This involves the use of naturally available biomaterials or their derivatives such as plants, bacteria, algae, viruses, fungi, phytoextracts, amino acids, sugar and glucose for preparation of stable nanoparticles [8-13]. Non-living biomasses or the phytoextracts possess the advantage of flexible handling of the material compared to the living biomasses. In addition, it can also be suitably scaled up for large-scale synthesis of NPs.

Herein, we have employed the aqueous extract of waste coconut coir biomass for the synthesis of AuNPs. *Cocos nucifera* Linn (Arecaceae), commonly known as coconut palm is considered as 'The Tree of Life' since almost each part of the plant is useful in one or the other way to the society. Coconut palm is grown in the tropical regions throughout the world. It is one of the most commercially important crops in India with the production of 13 billion nuts per annum, which corresponds to a major share of world's total production. The coconut fruit has three layers: exocarp, mesocarp and endocarp. The exocarp and mesocarp make up the husk of the coconut which contains fibers and corky tissues called pith. The separation of the fibers from the husk results in considerable amounts of agricultural waste coir pith in the coir processing industries. Any suitable commercial use for the daily output of coir pith waste in a defibering unit would be advantageous to the society in view of reduction of waste. Coir pith waste is a lignocellulosic material comprising various polyphenolic compounds. It consists of functional groups like carboxylic, hydroxyl and lactone, which show exchange/sorption properties due to their affinity towards metal ions [14]. Earlier, we have demonstrated the use of this agricultural solid waste material for bioremediation [15-19]. This report is an extension of our efforts to explore the potential of coir waste biomass for development of green synthetic strategy for MNPs.

A simple, one step, and room temperature synthesis of AuNPs by reducing  $\text{HAuCl}_4$  in the presence of coir extract is developed. The influence of different experimental factors such as % volume fraction of coir extract, concentration of metal precursor, contact time and solution pH on the formation of AuNPs has been studied to optimize the synthesis conditions. The physico-chemical characterization of the AuNPs has been carried out using a range of spectroscopic and microscopic techniques. The mechanistic aspect of the nanoparticles synthesis and their stabilization are also illustrated. In addition, the catalytic activity of the as synthesized AuNPs has been studied during reduction of 4-NP to 4-AP using sodium borohydride.

## **2. Materials and methods**

### *2.1. Materials*

Coir waste used in the present studies has been provided by Central Coir Research Institute, Kerala, India. The obtained material was repeatedly washed with deionized water to remove adhering dirt if any and soluble impurities. It was then air dried; crushed and sieved. The powdered biomass was stored in an airtight plastic container. All chemicals used were of analytical reagent grade. Chloroauric acid ( $\text{HAuCl}_4 \cdot 3\text{H}_2\text{O}$ ) was obtained from Sigma Aldrich with 99.99% purity. A stock solution of  $1 \times 10^{-2}$  M was prepared by dissolving the appropriate amount of  $\text{HAuCl}_4 \cdot 3\text{H}_2\text{O}$  in deionized water. All the glassware were cleaned with dil  $\text{HNO}_3$ ; rinsed thoroughly with deionized water and oven dried at  $60^\circ\text{C}$ . The water used throughout this investigation was reagent-grade water (Resistivity =  $18.2\text{M}\Omega\text{cm}$ ), produced using a Millipore Synergy UV® ultrapure water purification system from Millipore Ltd., USA.

### *2.2. Preparation of coir extract*

Microwave assisted digestion was used to produce aqueous coir extract. Microwave irradiation was carried out using Ethos One, High Performance Microwave Digestion System, Milestone, USA at  $200^\circ\text{C}$  with a precise control over the heating temperature. One gram of coir pith was suspended in 25 mL of deionized water in a

teflon container. Microwave power was adjusted to 700 W for attaining 200 °C temperature. The reactor was cooled after irradiation. The aqueous extract was separated by filtration using 0.2 µm membrane filter from the insoluble fractions and used further for synthesis of gold nanoparticles. The extract was stored in a refrigerator at 4 °C.

### *2.3. Synthesis of gold nanoparticles by coir extract*

In a typical experiment, 50 µL of  $1 \times 10^{-2}$  M Au solution was added to the solution containing 250 µL of coir extract (5% volume fraction) in 4.7 mL deionized water followed by gentle swirling. The formation of the AuNPs by reduction of HAuCl<sub>4</sub> with the coir extract was indicated by the color change of the reaction mixture from pale yellow to bright red. The as synthesized AuNPs were further purified by centrifugation several times to remove excess coir extract. Effect of coir extract on the nanoparticle synthesis was studied by varying the % volume fraction of coir extract from 2 to 8%, while keeping the gold concentration fixed at  $1 \times 10^{-4}$  M (50 µL of 0.01M Au in 5 mL) and time at 30 min. Alternatively in another experiment, the influence of gold precursor on the synthesis of nanoparticles was evaluated by varying the concentration of gold precursor from  $0.2 \times 10^{-4}$  to  $4 \times 10^{-4}$  M in the presence of 5% volume fraction of coir extract for 30 min. The kinetics of the synthesis was analyzed by measuring the absorbance of the reaction mixture from 1- 300 min, containing  $1 \times 10^{-4}$  M Au and 5% volume fraction of coir extract. At this reagent concentration, the pH of the reaction mixture was varied from 1 to 12 to study its effect on the formation of AuNPs. All the syntheses were carried out in triplicate.

### *2.4. Characterization*

The absorption spectra of the as synthesized AuNPs were recorded using a CARY-100 Conc UV-Vis spectrophotometer (Varian, Palo Alto, CA) in the wavelength range of 400-750 nm. X-ray diffraction (XRD) pattern of as synthesized AuNPs was recorded on RIGAKU-D/MAX-IIIC (3 kW) operated at 40 kV power using CuK $\alpha$  radiation ( $\lambda = 0.15418$  nm) over a  $2\theta$  range of 10°-90° with a step size of 0.02°. The sample was prepared by drop casting the aqueous dispersion of AuNPs over the specific glass microscopic slide followed by air drying. The XRD spectrum was recorded at room temperature. The surface morphology and the size of the AuNPs were analyzed using a transmission electron microscope (Libra 120 KeV Electron Microscope (Carl Zeiss)) at an accelerating voltage of 200 kV. The samples for TEM analysis were prepared by drop casting the AuNPs solution on a carbon-coated copper grid followed by drying in air at room temperature. The elemental constituents of coir extract mediated AuNPs were tested by EDX analysis. The sample was prepared by depositing the colloidal AuNPs on the aluminium foil and the EDX spectrum was recorded using a scanning electron microscope (Tescan Vega MV2300T/40). For FTIR analysis, the sample solution was dried onto a substrate and analyzed in the range of 4000 to 500 cm<sup>-1</sup> using FTIR BRUKER IFS 66V/S-Germany. Surface charge on the samples was determined using a MALVERN Zetasizer Nano ZS. The yield for the present synthetic strategy has been evaluated by determining the concentration of gold using atomic absorption spectrometry (AAS). The measurements were carried out using a continuum source flame atomic absorption spectrometer, Contra AA 300, Analytik Jena, Germany at 242.8 nm with air-acetylene flame.

### *2.5. Catalytic performance of AuNPs in the reduction of 4-nitrophenol (4-NP) to 4-aminophenol (4-AP)*

The catalytic activity of as synthesized AuNPs, was evaluated for the reduction of 4-NP to 4-AP using sodium borohydride. The reduction of 4-NP was observed through UV-Vis spectroscopy in the range of 200-700 nm at room temperature in 1 cm path length cuvette. In a typical experiment, 4 mL of aqueous solution containing 0.05 mM of 4-NP, 15 mM of NaBH<sub>4</sub> and 0.1 mL as synthesized AuNPs were taken in a cuvette and the reaction

was observed for 30 min. Two control experiments were carried out under identical conditions except the addition of AuNPs and NaBH<sub>4</sub> respectively. The absorption spectra of the reaction mixture at a fixed time interval were recorded and analyzed further.

### **3. Results and discussion**

#### *3.1. Preparation of coir extract*

The biomass extraction has been achieved by numerous techniques, which include liquid-solid extraction, liquid-liquid extraction, acid-base extractions, ultrasound extraction (UE), microwave assisted extraction (MAE) etc. Herein, we have chosen microwave assisted extraction technique as it offers several advantages over the other techniques such as rapid extraction rate, reduced extraction time, less energy intensive and reduced solvent consumption [20-22]. In the present studies, the aqueous extract of coir has been prepared at 200 °C. Precise control over the heating temperature can be obtained by adjusting the power of the microwave irradiation. We have also attempted the extraction of coir in aqueous medium using hot plate and conventional heating. However, the coir extract yielded using these methods, was required in higher quantities for metal ion reduction and the kinetics was found to be slow; hence the coir extract prepared using microwave assisted digestion was used for the synthesis of AuNPs for further experiments. The microwave irradiation not only accelerated the biomolecules extraction from the coir pith but also there was formation of concentrated aqueous extract. This was helpful to enhance the rate for nanoparticle formation with small quantities of extract (as discussed later).

#### *3.2. Green synthesis of AuNPs*

The synthesis of AuNPs was carried out by reducing chloroauric acid with coir extract at room temperature. There was spontaneous color change of the reaction mixture from pale yellow to red indicating the formation of AuNPs. This is confirmed by the characteristic absorption maximum at 530 nm for the suspensions, which is attributed to the surface plasmon resonance (SPR) band of the AuNPs arising due to collective oscillation of the conduction band electrons interacting with the electromagnetic component of the visible light. Figure 1 represents the schematic for the present synthetic strategy. The quantification of gold ion concentration using atomic absorption analysis demonstrated that more than 95% of Au (III) was reduced in the reaction. The synthesis was found to be simple, rapid and can be carried out at room temperature without any specialized equipments.

#### *3.3. Effect of reaction parameters on the synthesis of AuNPs*

To study the effect of reaction conditions on the synthesis of AuNPs, different parameters were varied and the optimum conditions were determined. Figure 2 shows the effect of different % volume fraction of coir extract (2-8%) on AuNPs formation at a fixed concentration of Au (III) solution ( $1 \times 10^{-4}$  M). It was observed that within a few minutes of mixing the reactants, all the solutions turned red in color, which leads to the appearance of an absorption peak in the UV-Vis spectra for all the solutions. The solutions numbered 2-6 showed the similar peak maxima in each corresponding spectrum. At higher % volume fraction (>6%) the signal was broadened with a red shift in the peak position suggesting the possible increase in the particle size. Similar observation was also reported in the case of synthesis of metal nanoparticles using a stem extract of *Breynia rhamnoides* [23]. The resultant increase in the particle size with the increase in coir extract may be due to the secondary reduction processes on the surface of the formed nuclei in the presence of higher concentration of reducing moieties. Hence, it can be concluded that the optimized volume fraction of coir extract can be kept within 5% for further evaluations.

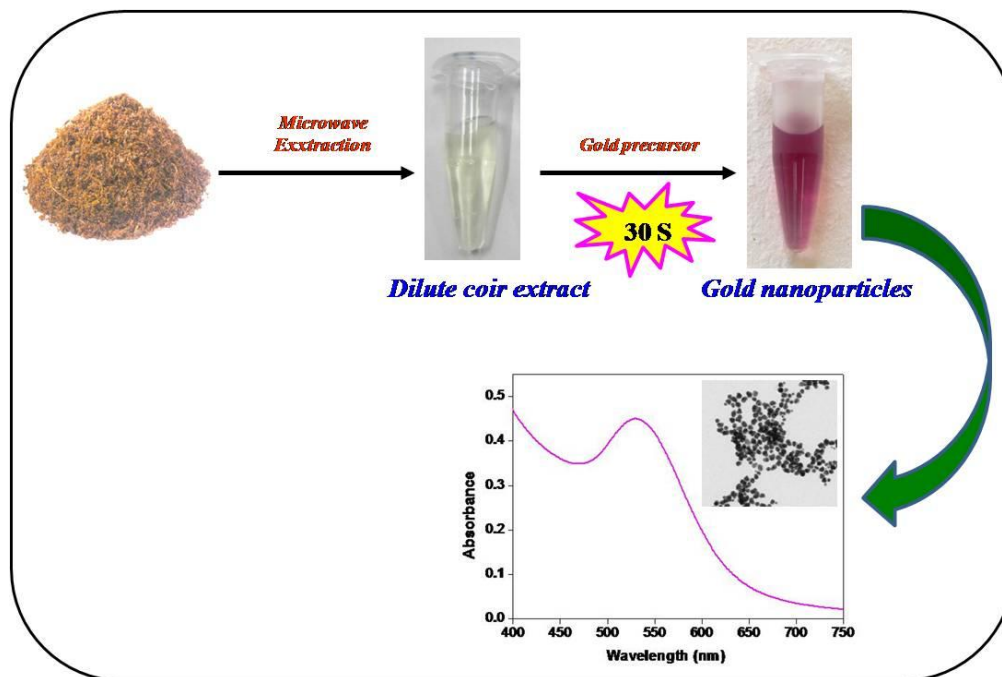


Figure 1: Schematic for the synthesis of gold nanoparticles using coir extract

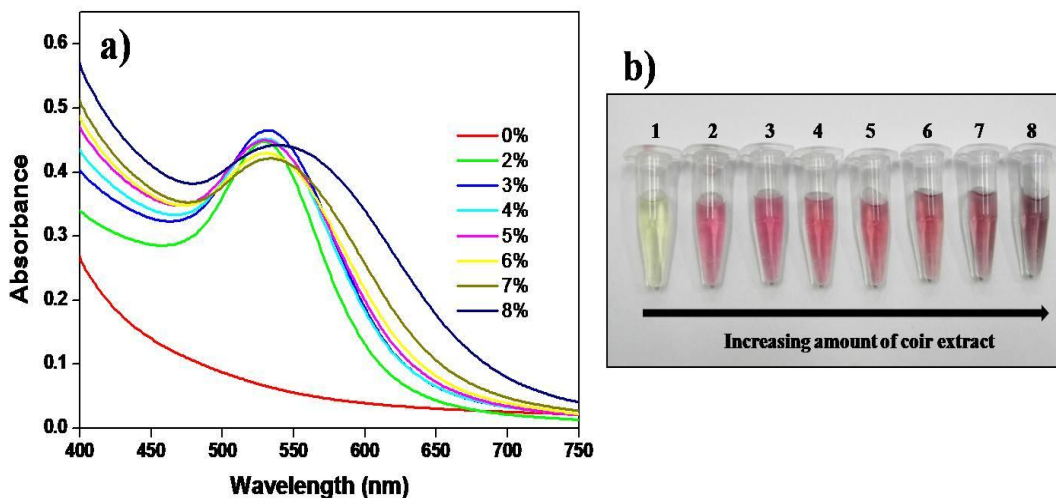
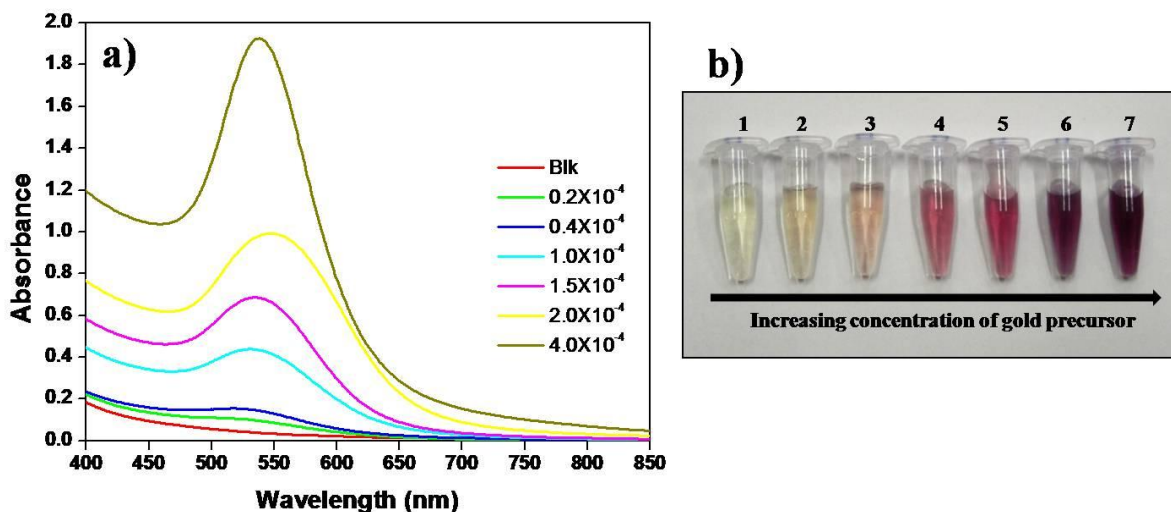


Figure 2: a) UV-Vis spectra of AuNPs synthesized using different amounts of coir extract while keeping the gold precursor concentration constant ( $1 \times 10^{-4}$  M) and b) Photographs of the solutions containing 1)  $\text{HAuCl}_4$  solution; 2-8) Colloidal AuNPs containing varying volume fractions of coir extract (2, 3, 4, 5, 6, 7 and 8% respectively)



**Fig**  
**ure 3:** a) UV-Vis spectra of AuNPs synthesized using different concentration of gold precursor while keeping the coir extract concentration constant (5% volume fraction) and b) Photographs of the solutions of colloidal AuNPs containing varying concentrations of gold precursor solutions 1-7) 0 to  $4 \times 10^{-4}$  M

In the next set of experiments, the concentration of gold was varied from  $0.2 \times 10^{-4}$  M to  $4 \times 10^{-4}$  M and the volume fraction of coir extract was kept constant at 5%. As shown in Figure 3, the color intensity of the solutions increased as the yield of the particles increased with increase in the metal precursor concentration. The observations were also supported by the UV-Vis spectra, which illustrated that there was an enhancement in the absorption signal intensity with increase in the concentration of gold precursor. This can be attributed to the high reduction capacity of the coir extract.

### 3.4. Kinetics studies

The kinetics of the reduction reaction was followed by monitoring the intensity of the SPR peak as a function of time. Figure 4 shows the UV-Visible absorption spectra of solution containing  $1 \times 10^{-4}$  M Au(III) and 5% volume fraction of coir extract at different time intervals. A distinct SPR peak was seen at 530 nm instantaneously after the addition of coir extract to gold salt solution indicating the rapid reduction of  $\text{HAuCl}_4$  to AuNPs. It was observed that the gold nanoparticle formation started instantaneously. The intensity of the absorption peak increased rapidly as a function of time with a negligible blue shift in the peak and reached to a maximum in 15 min. Increase in the absorbance indicated an enhancement in the reduction of gold ions with time. After 15 min, no further change in the spectrum was observed indicating the completion of the reduction reaction with consumption of precursors.

The narrowing or blue shift in the absorbance pattern with time indicates the size focusing of gold nanoparticles. The phenomenon of size evolution of nanoparticles can be explained by understanding the growth mechanism of the nanoparticles with time. Huang et. al [24] reported that the narrowing of particle size with time may be due to the two kinds of growth processes such as Ostwald ripening process and the self focusing enabled inter particle diffusion also known as intra particle ripening. Similarly in the present case, we envisage that Ostwald

ripening may dominate till the metal atoms have been exhausted completely after which there might be self focusing enabled inter particle diffusion. Thus both the growth processes may contribute towards formation of size limited particles and finally when the absorbance band is resolved completely, the average size of the particles is focused to a certain value. In general, the slower kinetics is a limitation for many intra- cellular and extra-cellular syntheses of nanoparticles [25-27]. Contrary to this, the present phytoextract mediated green synthesis method is quite rapid as compared to the other synthetic processes and proceeds without heating/stirring.

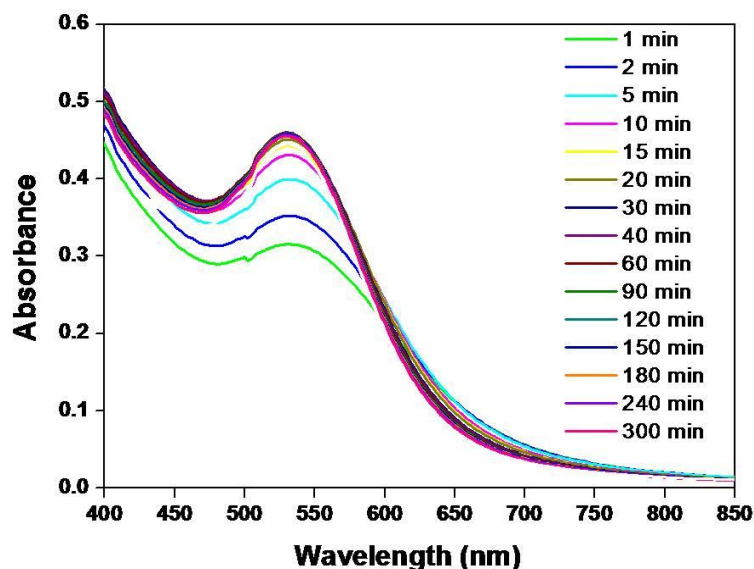


**Figure 4:** UV-Vis spectra of the solution containing  $1 \times 10^{-4}$  M of gold and 5% volume fraction of coir extract at fixed time intervals.

### 3.5. Effect of solution pH on the synthesis of AuNPs

Solution pH is one of the most important parameters in the synthesis of metal nanoparticles. The synthesis of AuNPs was carried out by varying the solution pH in the range of 1 to 12 with  $1 \times 10^{-4}$  M Au (III) and 5% volume fraction of coir extract. It was observed that the color of the solutions changed from pale yellow (pH 1) to greyish blue (pH 2); pink (pH 3-5); wine red (pH 6) and greyish violet (pH 7,8). However with further increase in the solution pH in highly alkaline region (pH 10-12), there was no color change observed for the solutions (Figure 5).

The corresponding UV-Vis spectra of all the solutions are presented in Fig. 5, which suggest that there was no formation of the AuNPs in the highly acidic (pH 1) and highly alkaline (pH 10-12) region. In the highly acidic region (pH 1), protonation of the phenolic groups occurs and hence reduction of Au(III) was not feasible. In highly alkaline (pH 10 to 12) region, phenolate anions are formed and hence no reduction takes place. At solution pH 2, the appearance of absorption peak in the region of 518 nm shows the initiation of AuNPs formation. With further increase in pH the in the range of 3 to 5 the absorbance maximum was observed at ~530 nm, which is the characteristic absorption peak for AuNPs as reported earlier. In higher solution pH (6 to 8), there was peak broadening with red shift in wavelength maxima, which may be due to the aggregation of AuNPs.

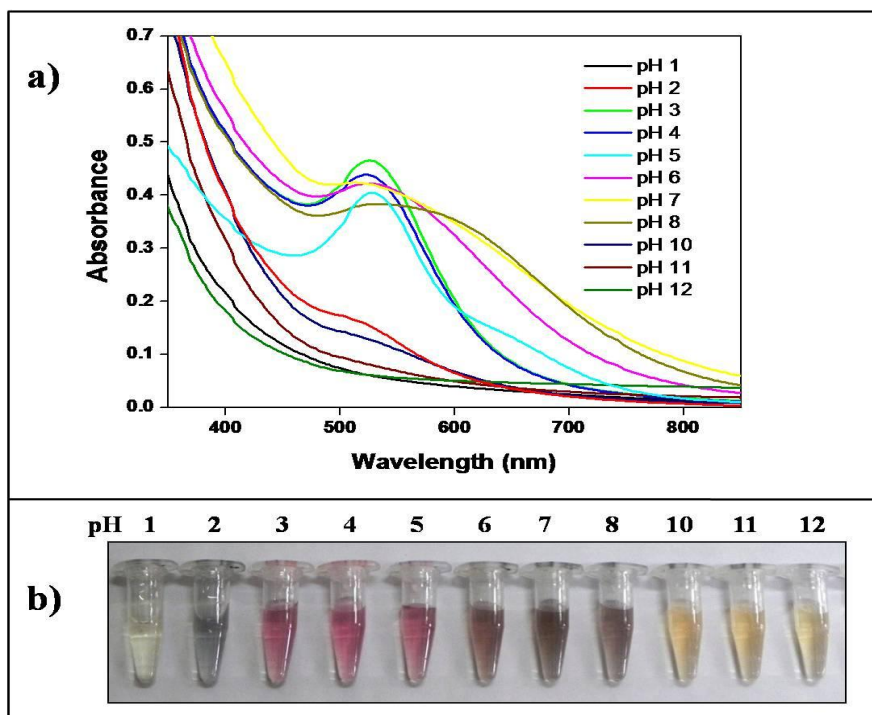


**Figure 5:** Influence of solution pH on the formation of AuNPs; a) UV-Vis spectra of the solutions containing  $1 \times 10^{-4}$  M of gold and 5% volume fraction of coir extract at different solution pH and b) Photographs of the corresponding solutions of colloidal AuNPs.

### 3.6. Characterization of AuNPs

The details of various analyses of as synthesized AuNPs are given as follows:

#### 3.6.1. Microscopic Analysis of surface morphology of AuNPs

The formation of AuNPs using coir extract was confirmed by TEM analysis. Figure 6a shows a typical TEM image of biosynthesized AuNPs with the corresponding size distribution histogram (Figure 6b). The 'ImageJ' software was used to analyze the particle size distribution and the resultant data were plotted in a histogram. It is clear from the Figure 6a, that the particles were predominantly spherical in shape. The particle size distribution was analyzed by considering more than 100 nanoparticles in the TEM image across the representative sample. The average particle size was found to be  $19.6 \pm 4.6$  nm. TEM analysis showed that the as synthesized particles were well dispersed without any sign of agglomeration, suggesting effective capping of the biomolecules present in the extract.

The elemental composition of the as-prepared AuNPs was evaluated by energy dispersive X-ray analysis (EDX). The spectrum (Figure 6c) shows strong characteristic peaks of Au along with some weak carbon and oxygen peaks. Since the excess coir extract (unbound biomolecules) was removed by centrifugation and repeated washings, the 'C' and 'O' signals obtained in the EDX spectrum are the signature of X-ray emissions from the biomolecules bound to the nanoparticles surface. EDX analysis confirmed the presence of 'Au' as the major element.

### 3.6.2. XRD Analysis

The crystalline nature of AuNPs was confirmed by analysis of XRD pattern as shown in Figure 6d. The XRD spectrum showed four distinct diffraction peaks at  $2\theta$  values of  $38.3^\circ$ ,  $44.4^\circ$ ,  $64.9^\circ$ , and  $78.1^\circ$  corresponding to the (111), (200), (220) and (311) lattice planes respectively. The comparatively larger peak intensity of the (111) plane indicated the predominant orientation of this plane. The analysis showed the evidence of the formation of face centered cubic (FCC) metallic gold; which were in good agreement with reference of FCC structure from joint committee of powder diffraction standard (JCPDS) file no. 04-0784.

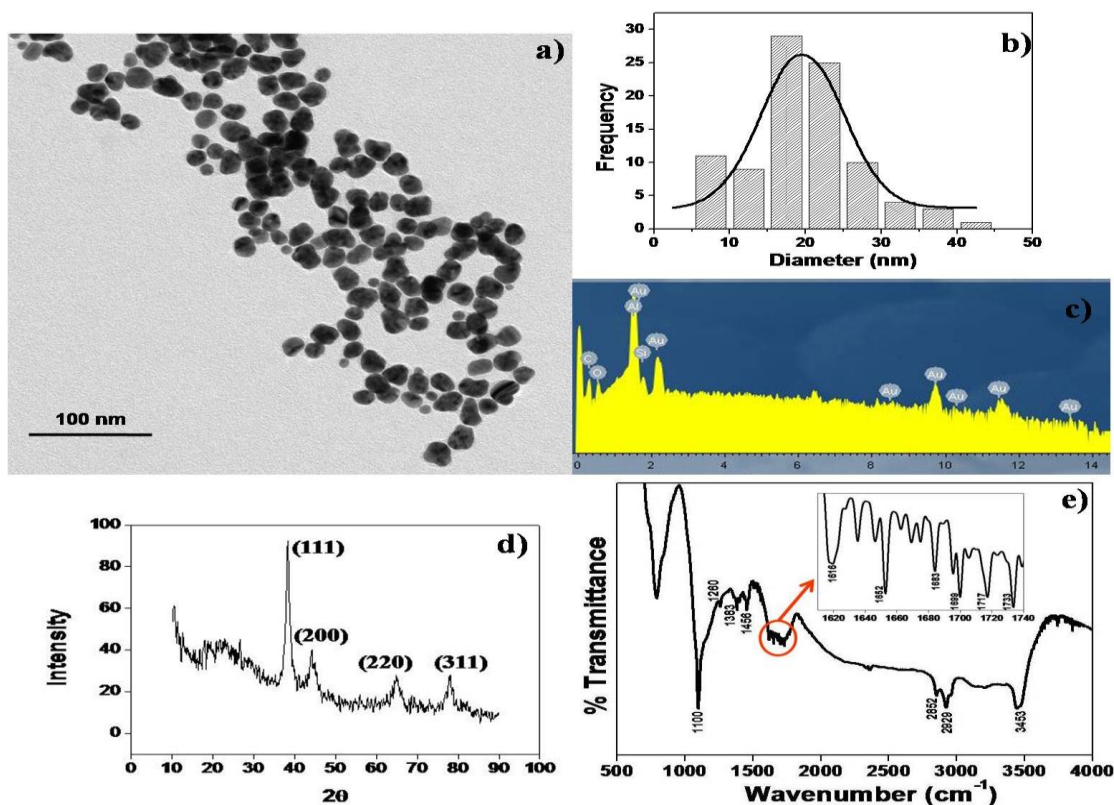


**Figure 6:** Characterization of AuNPs synthesized from coconut coir extract: a) TEM analysis; b) Size distribution histogram; c) EDX spectrum; d) XRD spectrum and e) FTIR spectrum.

### 3.6.3. FTIR Analysis

In order to determine a plausible mechanism for the AuNPs formation, it is important to identify the functional groups present in the coir extract, which are responsible for the reduction of metal ions and its stabilization. For this purpose, FTIR analysis of AuNPs formed using coir extract was carried out and the spectrum is shown in Figure 6e. The FTIR peak assignments for different functional groups are as follows [28,29]. The characteristic absorption bands present in the FTIR spectrum of coir extract were at  $3453$ ,  $2929$ ,  $2852$ ,  $1750$ - $1600$ ,  $1456$ ,  $1383$ ,  $1260$  and  $1100$   $\text{cm}^{-1}$  respectively. The band at  $3453$   $\text{cm}^{-1}$  can be attributed to the stretching vibration of hydroxyl (O-H) groups in the coir extract indicating the presence of polyphenols. The peaks at  $2929$   $\text{cm}^{-1}$  and  $2852$   $\text{cm}^{-1}$  can be assigned to the asymmetrical and symmetrical aliphatic C-H stretching vibrations. A clear broad dip in the region of  $1600$ - $1750$   $\text{cm}^{-1}$  is observed, which on close inspection (inset of Fig 6e) seems to be comprised of few shoulders at  $1733$ ,  $1717$ ,  $1699$ ,  $1683$ ,  $1652$  and  $1616$   $\text{cm}^{-1}$ . These shoulder peaks represent the

carbonyl stretching vibrations in ketones, carbonyls and ester groups. The peak at  $1456\text{ cm}^{-1}$  is assigned to the asymmetric bending in  $-\text{CH}_3$ ,  $-\text{CH}_2$  and carbohydrates. The peak at  $1383\text{ cm}^{-1}$  is assigned to the aliphatic C-H stretching in methyl and phenyl alcohols and bent modes of O-C-H, C-C-H, and C-O-H. The shoulder peak at  $1260\text{ cm}^{-1}$  can be caused due to the phenolic O-H and C=O stretching vibrations. The characteristic absorption peak at  $1100\text{ cm}^{-1}$  is attributed to the C-O, C-C and C-OH stretching vibrations. FTIR analysis thus indicates the presence of various functional groups (polyphenol moiety) from coir extract on the surface of nanoparticles; which might have involved in the bioreduction as well as stabilizing the AuNPs in aqueous medium.

Stability of the nanoparticles is an essential parameter in order to explore their possible applications. The conventional synthetic strategies for MNPs make use of different surfactants or polymers as stabilizers. In the present studies, the as synthesized AuNPs showed considerable stability without application of any external stabilizer upto 6 months as monitored by UV-Visible spectroscopy. About 5% decrease in the absorbance was detected after 6 months of storage of the AuNPs at ambient conditions. As per the above discussion, the FTIR spectrum indicated the capping of different functional groups on the surface of the AuNPs. Further to confirm this observation, we determined the surface charge of the AuNPs. The zeta ( $\zeta$ ) potential is commonly used to assess the stability of the colloidal systems. The results of  $\zeta$ -potential measurements revealed that the resulting AuNPs are negatively charged with a value of  $-20\text{ mV}$ . The high negative values of the zeta potential are due to the capping of phytoconstituents present in the extract. The electrostatic repulsive forces arising due to biocapping protect the AuNPs from getting closer to each other; thereby preventing their aggregation which lead to the considerable stabilization of the particles.

### *3.7. Mechanism of AuNPs formation*

Coconut coir is lignocellulosic in nature and hence there exist different functional groups such as carboxyl, hydroxyl and carbonyl in abundance. Earlier studies on compositional screening of coir extract have shown the presence of a variety of phytochemicals mainly a large number of polyphenols such as tannins, flavanoids and phenolic acids [30-32]. Polyphenolic compounds found in the plant materials are often found to play a key role in synthesis of nanoparticles by acting as reducing agents, metal chelators and singlet oxygen quenchers, thereby facilitating the reduction and stabilization of MNPs. Polyphenols exhibit strong antioxidant activity due to additional conjugation in the side chain, which assist the electron delocalization, by resonance and are able to donate electron or hydrogen atom.

During the present synthesis, Au (III) can form complexes with phenolic  $-\text{OH}$  groups present in the coir extract, which upon subsequent reduction are converted to elemental gold with simultaneous oxidation of hydroxyl groups to carbonyl groups (Figure 7). The  $\text{Au}^0$  atoms may collide with each other to form AuNPs. The initially formed AuNPs act as the seeds for further nucleation and growth of nanoparticles. The excessive biomolecules in the solution may interact with the surface atoms of AuNPs via its adjacent hydroxyls, thereby contributing to the stabilization of AuNPs. Electrostatic repulsion due to negative charge on the biomolecules is the main stabilization factor for AuNPs. Additionally the steric bulk of the backbone of the quinone derivatives and other phytochemicals wrapping around the nanoparticles provide robustness against further aggregation of the stabilized AuNPs. Gan et al has also reported the gold ion complexation by hydroxyl groups from the palm oil mill effluent (POME) and its subsequent bioreduction through oxidation of hydroxyl to carbonyl groups [33]. In another report of silver ion bioreduction by Gum kondagogu, a natural biopolymer, the authors propose that during processes there can be oxidation of the existing hydroxyl groups to carbonyl groups such as aldehydes and carboxylates due to the dissolved air [29]. These aldehydes along with the other existing abundant carbonyl groups reduce more gold ions to elemental gold.

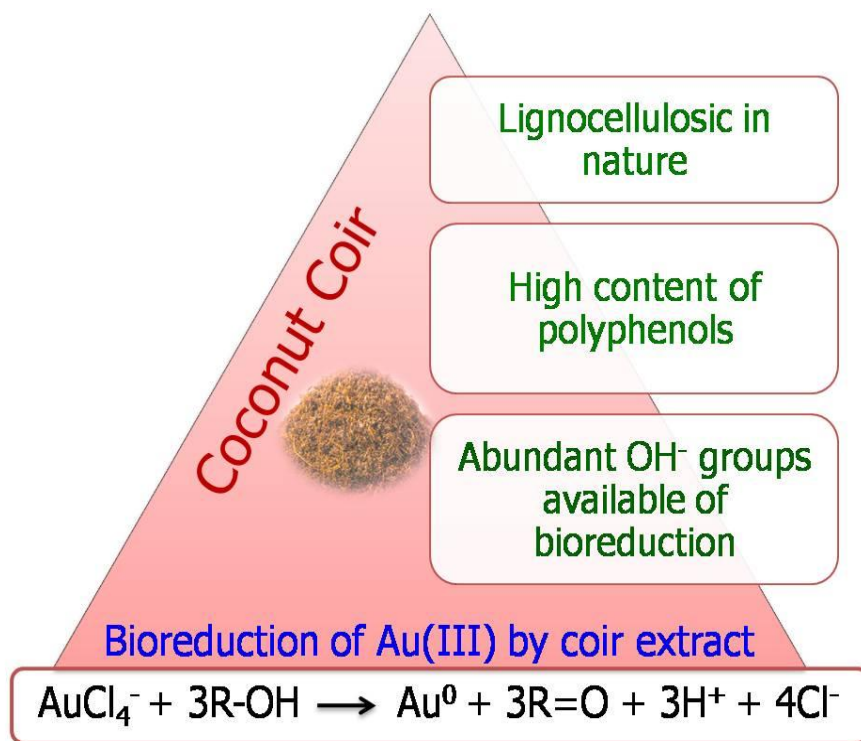


Figure 7: Mechanism of AuNPs formation

### 3.8. Catalytic performance of AuNPs in the reduction of 4-nitrophenol (4-NP) to 4-aminophenol (4-AP)

Earlier reports have shown that AuNPs are catalytically active for several chemical reactions [34-40]. In the present studies, we have made an attempt to investigate the catalytic activity of as synthesized AuNPs for a model reaction of reduction of 4-NP to 4-AP in the presence of sodium borohydride. The reaction was analyzed by measuring the absorbance of the reaction mixture in the wavelength range of 200-700 nm for fixed time intervals (Figure 8a-b). Initially, the absorption spectra of 4-NP (0.05 mM) showed the absorption peak at 317 nm, which upon addition of excess NaBH<sub>4</sub> (15 mM) shifted to longer wavelength at 400 nm due to the formation of 4-nitrophenolate anion under basic conditions. This was also observed by a quick change in the solution color to bright yellow after addition of NaBH<sub>4</sub> to 4-NP. Further, the addition of AuNPs to the reaction mixture resulted in bleaching of the yellow color of the solution with time, which leads to decrease in the absorption intensity of the peak at 400 nm along with appearance of a new peak at 300 nm corresponding to the formation of 4-AP. The kinetics of the reduction was followed by monitoring the absorbance spectrum of the reaction mixture for 30 min (Figure 8b). The reduction reaction was completed in 10 min at room temperature with associated color change of the solution from bright yellow to colorless.

However, the control experiment performed in the absence of AuNPs catalyst, showed that reaction solution retained the bright yellow color with a constant absorption peak at 400 nm due to nitrophenolate ion. There was not much change in the absorption spectra of the mixture in this period suggesting reduction of 4-NP did not proceed in the absence of added catalyst. Similarly, in the second control experiment, performed in the absence of NaBH<sub>4</sub>, the absorbance pattern of 4-NP was found to be identical after the addition of AuNPs with a constant peak maxima at 318 nm, when monitored for 30 min. This suggest that the reduction of 4-NP did not take place

in the absence of  $\text{NaBH}_4$ . Though the reduction of 4-NP to 4-AP is thermodynamically possible using  $\text{NaBH}_4$ , there was no change in the absorption spectrum of the reaction mixture (in the absence of AuNPs) on standing for a long time due to the kinetic barrier. However, in the presence of AuNPs the reaction was completed in a few minutes.

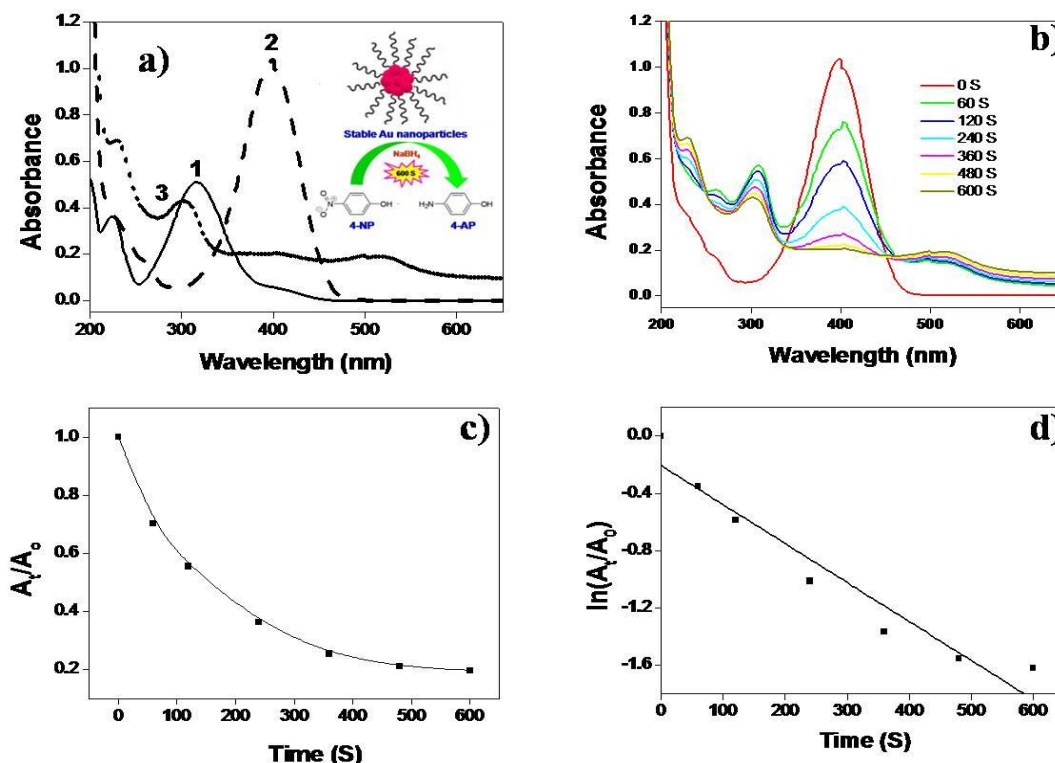


**Figure 8:** Study of catalytic activity of AuNPs during reduction of 4-NP to 4-AP in the presence of  $\text{NaBH}_4$ ; a) UV-Vis spectra of 1) 4-NP (0.05mM); 2) 4-NP in the presence of presence of  $\text{NaBH}_4$  (15nmM); and 3) after complete reduction of 4-NP in the presence AuNPs as catalyst (Inset shows the schematic representation of the catalytic reduction of 4-NP to 4-AP) b) Time dependent UV-Vis spectra of the for the reduction of 4-NP catalyzed with AuNPs in the presence of  $\text{NaBH}_4$ ; C) and D) plot of  $A_t/A_0$  and  $\ln(A_t/A_0)$  Vs time for the reduction of 4-NP with AuNPs respectively.

The hydroxyl groups from polyphenols associated with the AuNPs are responsible for drawing the electron donor  $\text{BH}_4^-$  and electron acceptor 4-nitrophenolate ion near to the surface of AuNPs and consequently their adsorption on the surface of AuNPs. Further, the catalytic activity of AuNPs mediates the passage of electrons from sodium borohydride donor to the acceptor molecules of 4-NP which result in initiation of the conversion reaction. Thus the AuNPs lowers the activation energy and facilitates the reduction of 4-NP; thereby playing the role as a catalyst.

The present catalytic reduction of 4-NP to 4-AP was carried out in the presence of  $\text{NaBH}_4$ . It is assumed that the concentration of  $\text{NaBH}_4$  remains constant during the progress of the reaction and the reaction is considered to be pseudo first order kinetics with respect to 4-NP. The rate determining step is the surface reaction of both 4-NP and sodium borohydride and the reaction continues till the complete consumption of 4-NP. After the reaction the product 4-AP gets desorbed from the catalyst AuNPs surface and the free active sites are formed for further adsorption of reactants. The reaction continues till the complete consumption of 4-NP. The reaction progress

was examined spectrophotometrically at different time intervals and the catalytic reaction rate constant was calculated. Fig. 8c shows the plot of  $A_t/A_0$  against time during the reduction of 4-NP, where  $A_t$  is the absorbance at the designated time and  $A_0$  is the initial absorbance at  $t=0$ . A linear correlation of  $\ln(A_t/A_0)$  vs  $t$  (Figure 8d) was obtained, which supported our assumption of pseudo first order kinetic rate model. The rate constant ( $k$ ) calculated from the slope of the plot is found to be  $2.73 \times 10^{-3} \text{ s}^{-1}$ . The obtained value of  $k$  is found to be comparable with the other reported rate constants for the similar reaction. Moreover, further increase in the catalytic rate constant would be possible with the increase in the concentration of the AuNPs as the number of active sites available for the reaction would increase.

From all the above discussion, it is important to highlight the advantages of the present synthetic strategy. The synthesis is one step, simple, rapid, can be performed at ambient temperature and pressure without any special equipments and results in stable nanoparticles. Coir extract acts as both reducing agent and stabilizer during the synthesis process. The synthesis is ecofriendly with excellent reproducibility and high yield and there is no toxic waste generated. The synthesis can be implemented for the large scale production of monodispersed and spherical nanoparticles due to the availability of waste coir biomass. The synthesis could be extended for generation of various other metal nanoparticles.

## Conclusions

A one step, rapid and environmental friendly room temperature synthesis of AuNPs using coir extract is developed. The coir extract acted as both reducing agent and stabilizer during the AuNPs formation. The water soluble polyphenols present in the coir extract are responsible for the reduction of gold (oxidation of phenolic groups to quinone with consequent reduction of  $\text{Au}^{3+}$  to  $\text{Au}^0$ ). The synthesized AuNPs were predominantly spherical in shape with an average size of  $19.6 \pm 4.6 \text{ nm}$ . AuNPs were negatively charged with a zeta potential of  $\sim 20 \text{ mV}$ , which suggest the stable dispersion of AuNPs in medium. The AuNPs showed excellent catalytic activity during the reduction of 4-NP to 4-AP in the presence of sodium borohydride.

**Acknowledgements**-Authors would like to thank Dr. Anand Ballal for TEM analysis; Dr. Shovit Bhattacharya for EDX analysis; Dr. Awadesh Kumar for FTIR analysis and Dr. M. R. Gonal for XRD analysis.

## References

1. Daniel M. C., Astruc D. *Chem. Rev.* 104 (2004) 293.
2. Hu M., Chen J., Li, Z. Y., Au L., Hartland G. V., Li X., Marquez M., Xia Y., *Chem. Soc. Rev.* 35 (2006) 1084.
3. Jain P. K., Huang X., El-Sayed I. H., El-Sayed M. A., *Accounts Chem. Res.* 41 (2008) 1578.
4. Turkevich J., Stevenson P. C., Hillier J., *Discuss. Faraday Soc.* 11 (1951) 55.
5. Dahl J. A., Maddux B. L. S., Hutchison J. E., *Chem. Rev.* 107 (2007) 2228.
6. Brust M., Walker M., Bethell D., Schiffrin D. J., Whyman R., *Journal of the Chemical Society, Chem. Commun.* (1994) 801.
7. Frens G., *Nature Physical. Sci.* 241 (1973) 20.
8. Hebbalalu D., Lalley J., Nadagouda M. N., Varma R. S., *ACS Sustainable Chem. Eng.* 1 (2013) 703.
9. Akhtar M. S., Panwar J., Yun Y. S., *ACS Sustainable Chem. Eng.* 1 (2013) 591.
10. Baker S., Rakshith D., Kavitha K. S., Santosh P., Kavitha H. U., Rao Y., Satish S., *BioImpacts* 3 (2013) 111.

11. Dubey S. P., Dwivedi A. D., Lahtinen M., Lee C., Kwon Y. N., Sillanpaa M., *Spectrochim. Acta Part A* 103 (2013) 134.
12. Mittal A. K., Chisti Y., Banerjee U. C., *Biotechnol. Adv.* 31 (2013) 346.
13. Mohamad N. A. N., Arham N. A., Jai J., Hadi A., *Adv. Mater. Res.* 832 (2014) 350.
14. Tan W. T., Ooi S. T., Lee C. K., *Environ. Technol.* 14 (1993) 277.
15. Parab H., Joshi S., Shenoy N., Lali A., Sarma U. S., Sudersanan M., *Process Biochem.* 41 (2006) 609.
16. Parab H., Joshi S., Shenoy N., Lali A., Sarma U. S., Sudersanan M., *Bioresour. Technol.* 99 (2008) 2083.
17. Parab H., Joshi S., Shenoy N., Verma R., Lali A., Sudersanan M., *Bioresour. Technol.* 96 (2005) 1241.
18. Parab H., Sudersanan M., *Water Res.* 44 (2010) 854.
19. Parab H., Sudersanan M., Shenoy N., Pathare T., Vaze B., *Clean - Soil, Air, Water* 37 (2009) 963.
20. Ballard T. S., Mallikarjunan P., Zhou K., O'Keef, S., *Food Chem.* 120 (2010) 1185.
21. Japón-Luján R., Luque-Rodríguez J. M., Luque de Castro M. D., *Anal. Bioanal. Chem.* 385 (2006) 753.
22. Tsubaki S., Iida H., Sakamoto M., Azuma J. I., *J. Agric. Food Chem.* 56 (2008) 11293.
23. Gangula A., Podila R. M. R., Karanam L., Janardhana C., Rao A. M. , *Langmuir* 27 (2011) 15268.
24. Huang J. H., Parab H. J., Liu R. S., Lai T. C., Hsiao M., Chen C. H., Sheu H. S., Chen J. M., Tsai D. P., Hwu Y. K. *J. Phys. Chem. C* 112 (2008) 15684.
25. Kitching M., Ramani M., Marsili E., *Microb. Biotechnol.* 8 (2015) 904.
26. Sadowski Z. (2010) Biosynthesis and Application of Silver and Gold Nanoparticles, Silver Nanoparticles, David Pozo Perez (Ed.), ISBN: 978-953-307-028-5, In Tech publications, Croatia.
27. Singh O. V. (2015) Bio-Nanoparticles: Biosynthesis and Sustainable Biotechnological Implications, Wiley Blackwell, published by John Wiley and Sons Inc., Hoboken, New Jersey.
28. Harshala Parab, P. S. Remya Devi, Niyoti Shenoy, Sangita D. Kumar, Y. K. Bhardwaj, A. V. R. Reddy, *J. Radioanal. Nucl. Chem.* DOI 10.1007/s10967-015-4569-4.
29. Kora A.J., Sashidhar R.B., Arunachalam J., *Carbohydr. Polym.* 82 (2010) 670.
30. Bankar G.R., Nayak P.G., Bansa, P., Paul P., Pai K.S.R., Singla R.K., Bhat V.G., *J. Ethnopharmacol.* 134 (2011) 50.
31. Chakraborty M., Mitra A., *Food Chem.* 107 (2008) 994.
32. Israel A.U., Ogali R.E., Akaranta O., Obot I.B., *Songklanakar J. Sci. Technol.* 33 (2011) 717.
33. Gan P.P., Ng S.H., Huang Y., Li S.F.Y., *Bioresour. Technol.* 113 (2012) 132.
34. He W., Zhou Y.T., Wamer W.G., Hu X., Wu X., Zheng Z., Boudreau M.D., Yin J.J., *Biomater.* 34 (2013) 765.
35. Hvolbæk B., Janssens T.V.W., Clausen B.S., Falsig H., Christensen C.H., Nørskov J.K., *Nano Today* 2 (2007) 14.
36. Jaramillo T.F., Baeck S.H., Cuenya B.R., McFarland E.W. , *J. Am. Chem. Soc.* 125 (2003) 7148.
37. Lee Y., Loew A., Sun S., *Chem. Mater.* 22 (2010) 755.
38. Wu X. , Lu C. , Zhou Z. , Yuan G. , Xiong R. , Zhang X., *Environ. Sci. Nano*, 1 (2014) 71.
39. Sen I.K., Maity K., Islam S.S., *Carbohydr. Polym.* 91 (2013) 518.
40. Das S.K., Dickinson C., Lafir F., Brougham D.F., Marsili E., *Green Chem.* 14 (2012) 1322.

(2016) ; <http://www.jmaterenvironsci.com>